EIR-Bericht Nr. 329

EIR-Bericht Nr. 329

Eidg. Institut für Reaktorforschung Würenlingen
Schweiz

Monte-Carlo-Transport Studies in the HHT Primary Circuits

A. Taormina, S. Kypreos

Würenlingen, October 1977

MONTE CARLO TRANSPORT STUDIES IN THE HHT PRIMARY CIRCUITS

A. Taormina, S. Kypreos

Würenlingen, September 1977

C o n t e n t s :

Abstract

This report describes the calculation of neutron and gamma ray fluxes and dose rates in the Helium ducts and the Turbomachinery of various HHT* designs. The PCRV geometry and the arrangement of the Helium Turbines is described and the different material specifications are summarised. The neutron source at the upper level of the gas plenum is defined using the discrete ordinates approximation of the transport equation in the reactor core. The complicated shielding requires an exact three dimensional solution of the neutron and gamma ray transport. This is obtained using the Monte Carlo program FMCEIR which is briefly described. Neutron fluxes are given. Dose rates are calculated during operation and two days after shut-down. The effectivness of a boronate graphite wall to attenuate the neutron flux and to reduce the dose rate is also examined. The source is devided into different energy groups to study how the calculated results are affected by the thermal, epithermal and fast source neutrons. The variance is calculated by grouping the histories and the Shapiro-Wilk normality test is performed.

* HHT = High Temperature Reactor with Helium Turbine

1. Introduction

The High Temperature Gas Cooled Reactors have some unique characteristics: Their safety is enhanced due to the high heat capacity of the ceramic core and the prestressed concrete reactor vessel (PCRV). Their high gas outlet temperature make them potential candidates for process heating applications. They could obtain the best utilisation of thorium resources between the thermal reactors and also they possess a unique flexibility to change their fuel cycle during operation. Finally a potential application of the system is the use of gas turbines (or combined gas and steam cycles) to achieve even higher efficiencies for electricity production. All these advantages should result in the commercialization of the system in the next decades.

Due to these unique advantages and the broad spectrum of applications of the system, a cooperative study has been undertaken between the Federal Republic of Germany and Switzerland for the development of a High Temperature Reactor with Helium Turbine (HHT). In terms of this project a study is described here to calculate the neutron streaming along the hot gas ducts of the PCRV and the gamma ray dose rate in the turbogroups to ensure their accessibility. Two different HHT concepts have been investigated in which the effectiveness of the shielding and the boronate graphite wall to attenuate the neutrons and to reduce the dose rate is examined. Due to the deep penetration inside the PCRV and the complexity of the three dimensional geometry the Monte Carlo method has been selected, while one dimensional discrete ordinates transport calculations are performed to define the source.

2. General description of the Monte Carlo Program FMCEIR and its library

The FMCEIR is an extended and improved version of the "Flexible Monte Carlo program FMC" which was originally developped by General Electric[1]. The new version is described in ref. 2. The program simulates the neutron and gamma ray histories in a source-shielding configuration. There is a flexibility in the geometrical, nuclear, source description and variance reduction techniques used. Energy and geometry restart options are available, while subroutines to plot the geometrical configuration, to combine linearly a set of runs, to check for normality, to calculate the variance and to plot the results are now in use. Neutron upscattering could be optionally treated in connection with the energy restart option. The program is using an extension of the track length estimator to calculate the region fluxes, while region and energy importance, splitting, Russian roulette and exponential transformation could be used optionally to reduce the variance.

The ENDF/B files version III, was used as basic information to evaluate the FMCEIR library of cross sections. The ultrafine option of MC2[3,4] is utilised to calculate the neutron spectrum and to collapse the basic data to a desirable number of groups. The complete set of tabulated Legendre Coefficients in ENDF/B files are used to calculate the secondary angular distribution, while the P_o MC2 scattering matrices give the secondary energy distribution. The thermal range is covered by a library of 123 groups produced by FLANGE or the free gas model[5]. These data were condensed into fewer groups using a maxwellian spectrum. The neutrons propagated through the shielding configuration are generating gamma rays. The gamma ray production data are calculated with LAPHANO[6,7] and MC2.

Finally the gamma ray interaction data are produced with SMUG[8,9]. The general procedure to calculate the libraries of FMCEIR is shown in the flow diagram of Fig. 1. To verify the libraries and the program a set of theoretical and experimental benchmarks have been recalculated. Ref. (10) gives the results of an intercomparison between the program FMCEIR, MORSE and DOT concerning neutron streaming along a sodium duct. Ref. (11) and (12) give the results of a comparison with experiment for gamma and neutron flux in multi-legged concrete ducts.

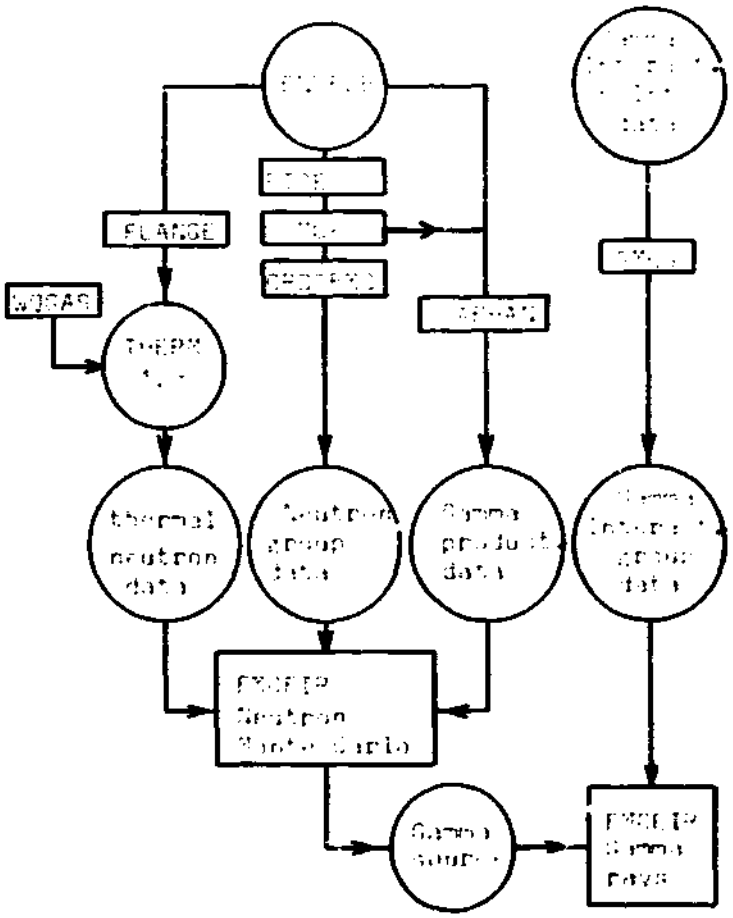

Fig.1 General organisation of the programs and basic data used to produce the libraries of FMCEIR

3. Description of the problem to be calculated

3.1. General

The reactor building of the HHT plant contains the prestressed concrete reactor vessel. The PCRV encloses the reactor, the primary coolant system, the heat exchanger components and the turbogroups. The PCRV is made gas-tight by means of an inner steel liner, supplemented by thick concrete walls. Two different concepts of the primary coolant system are investigated here. The standard HHT design has three main loops, each with independent turbogroups and heat exchangers without intercoolers. The second design has only one loop. The hot gas is seperated into two paths which enter one turbine located below the core. After the expansion the gas is directed to the recuperator, precooler and to the compressor with intercooler. It returns then to the core, split into two paths through the recuperators, coaxial to the hot gas.

3.2 Simulation of geometry by PMCEID

An effort has been made to simulate exactly the geometry of the HHT with emphasis on the twin gas ducts, the gas plenum and the openings of the boronate graphite wall, examining the neutron streaming along them. Due to the existing symmetry of the standard three loop design only a sector of 120^{o} is treated. This sector was bounded by reflecting planes. The coolant flows down through the core and bottom reflector to the gas plenum. Through the openings of the boronate graphite wall it enters the horizontal hot ducts moving towards the gas turbine. This duct is curved after 3.75 m. The vertical length of the duct until gas turbine

inlet is 4.6 m. The vertical part of the duct is coaxially housed inside another thicker duct. This outside duct directs the cold gas flow. The one loop design has a symmetry of 180°. The hot duct has a double bend. The vertical length of the duct is 9 m while the turbine is located below the core in a distance of 9 m from the vertical duct. The total length of this duct is about 21 m. The cold gas ducts are always coaxially enclosing the hot ducts. Fig.2 gives vertical and horizontal section of the three loop design as it is simulated by FMCEIR. Similar sections are given in Fig.3 for the one loop design. The smeared densities used in the calculations for the duct walls, the boronate shielding wall, the insulation, the PCRV and the turbine are given in table 1.

3.3 Definition of the neutron source

The energy space and angle distribution of the Monte Carlo source are defined using the results of ANISN.

The ANISN calculations are based on the core dimensions and material composition of a standard HTGR design. The P_3-S_8 approximation was used in the range between 15 MeV - 41 KeV. The rest of the spectrum was calculated in P_0-S_2 with upscattering in the thermal range. The calculations were performed by HRB (Hochtemperatur-Reaktorbau GmbH, BRD). Fig.4 gives the neutron flux distribution in four broad energy ranges, as it was calculated by ANISN (as function of the distance from the core middle plane). The source was located in the upper part of the gas plenum and it was assumed uniformly distributed in an area of radius 420 cm. The directional flux distribution calculated by ANISN is given in Fig.5 and Fig.6 for the different energy groups. The

anisotropy is decreasing with decreasing neutron energy. The azimuthal distribution was assumed isotropic. The total fluxes were normalised to get the fraction of neutrons per group, while inside the group the neutrons have isotropic distribution.

Table 1 Atom densities used (atoms/barn·cm)

Nuclides	Concrete	Duct wall	Boronated wall	Insulation	Turbine
O	4.42 E-2			1.37 E-2	
Si	1.59 E-2	5.5 E-4		6.52 E-3	6.71 E-4
H	8.00 E-3				
Ca	2.94 E-3				
Al	2.41 E-3	1.72 E-4		4.26 E-4	
Na	1.06 E-3				
K	7.00 E-4				
Fe	3.10 E-4	4.71 E-2		2.50 E-3	8.24 E-2
Mg	1.40 E-4				
Ni		2.67 E-2			
Cr		6.14 E-3			9.07 E-4
C		4.78 E-4	8.12 E-2	1.70 E-5	5.89 E-4
B_{10}		3.93 E-6	3.61 E-4		
B_{11}		1.54 E-5	9.20 E-5		
Mo		3.76 E-3			1.97 E-4
Mn		3.25 E-4		1.10 E-5	3.43 E-4

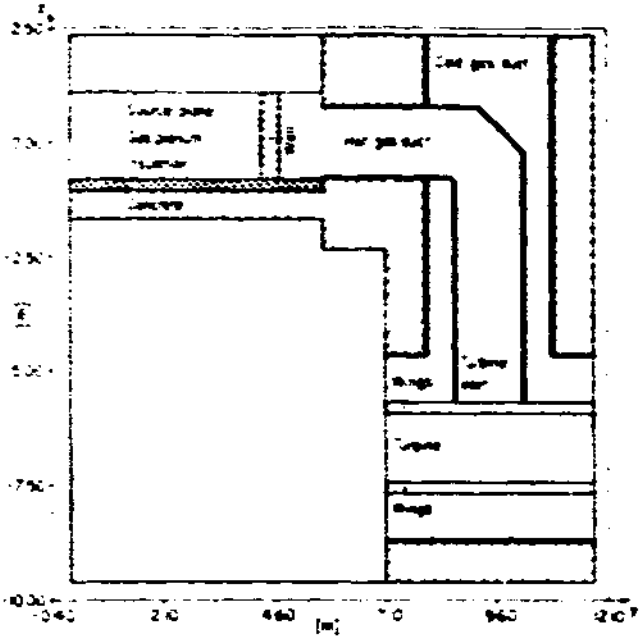

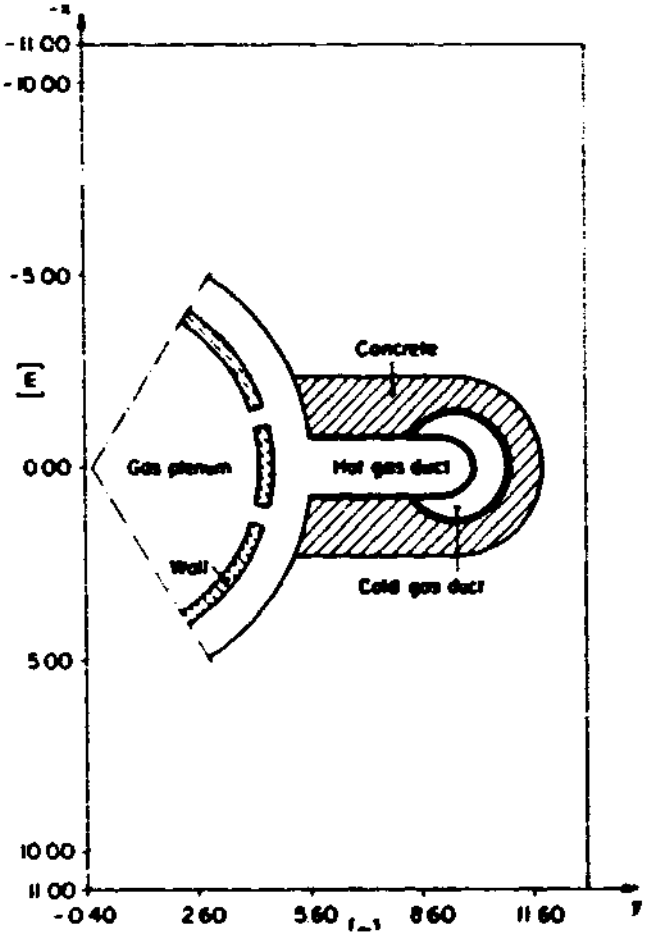

Fig. 2 Vertical and horizontal section of the three loop design as simulated by FMCEIR

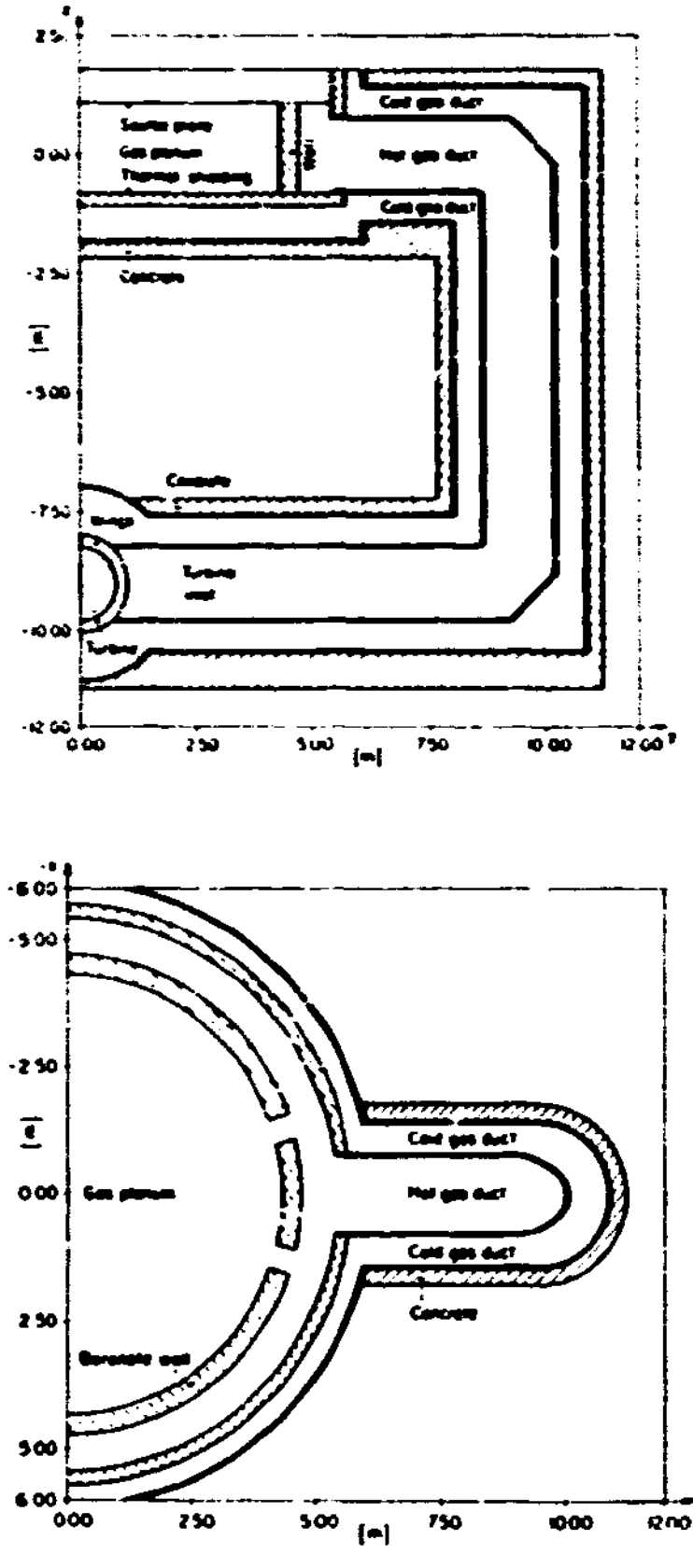

Fig. 3 Vertical and horizontal section of the one loop design as simulated by FMCEIR

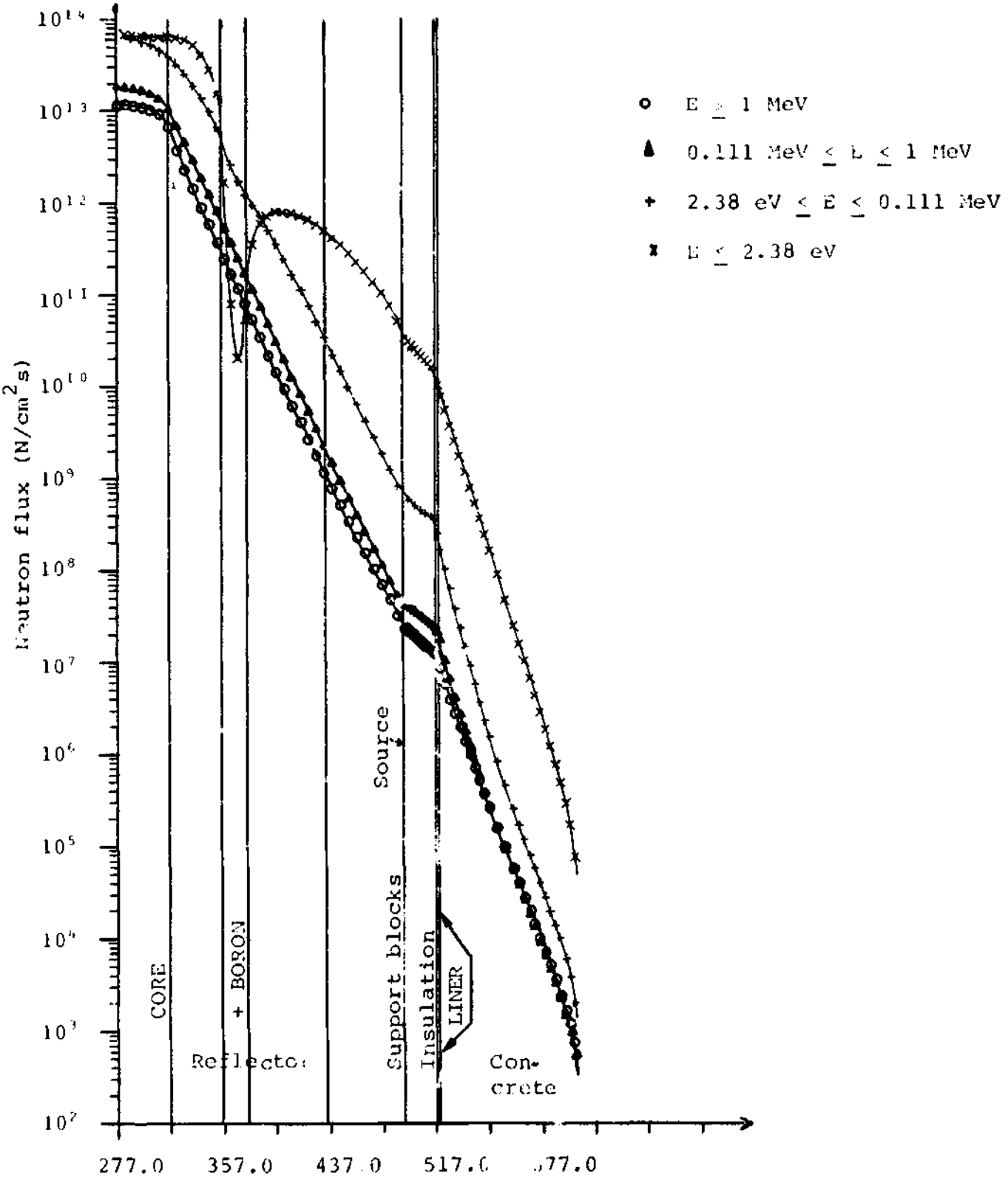

Fig. 4 Neutron flux distribution at the upper part of the gas plenum

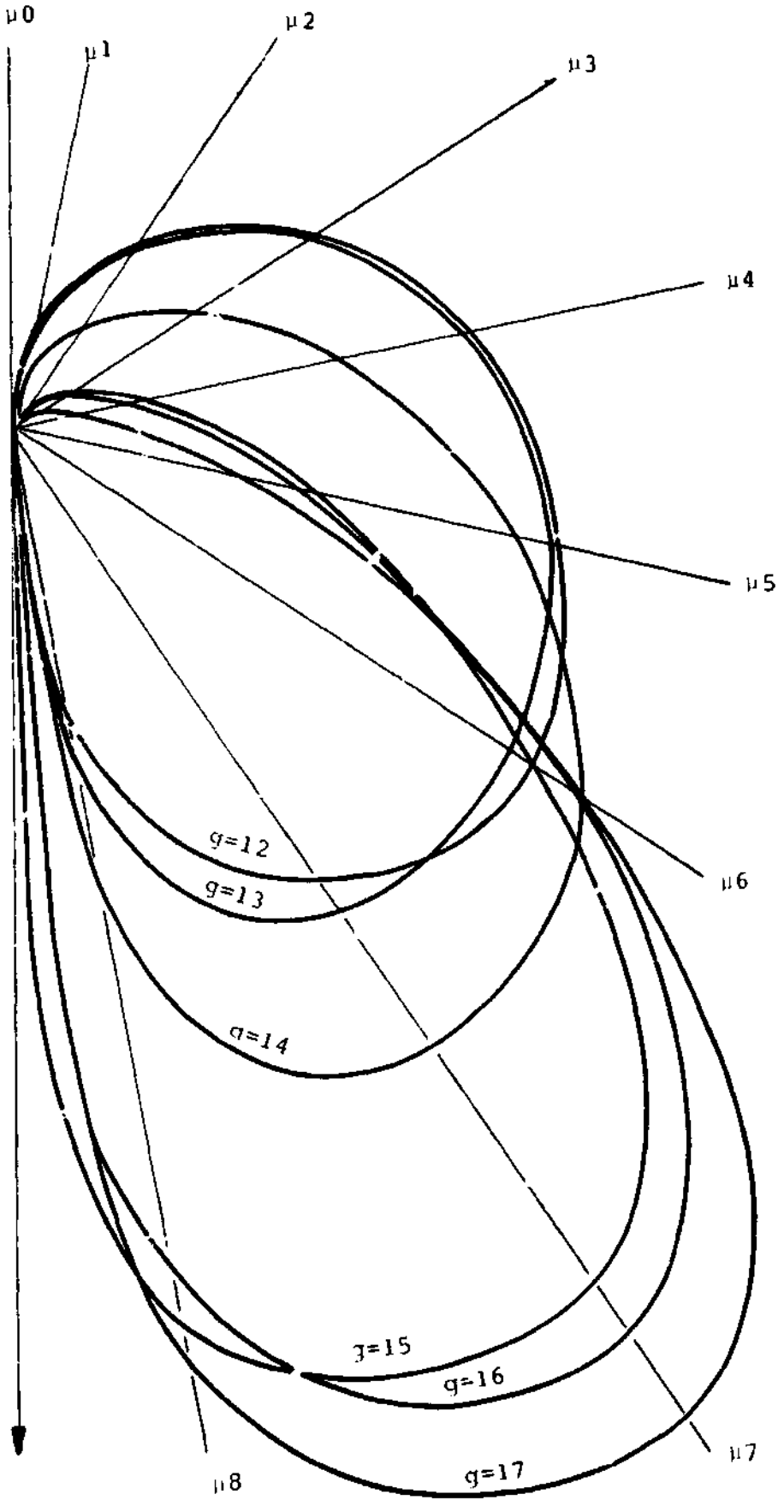

Fig. 5 Directional flux distribution for the energy groups 17 - 12

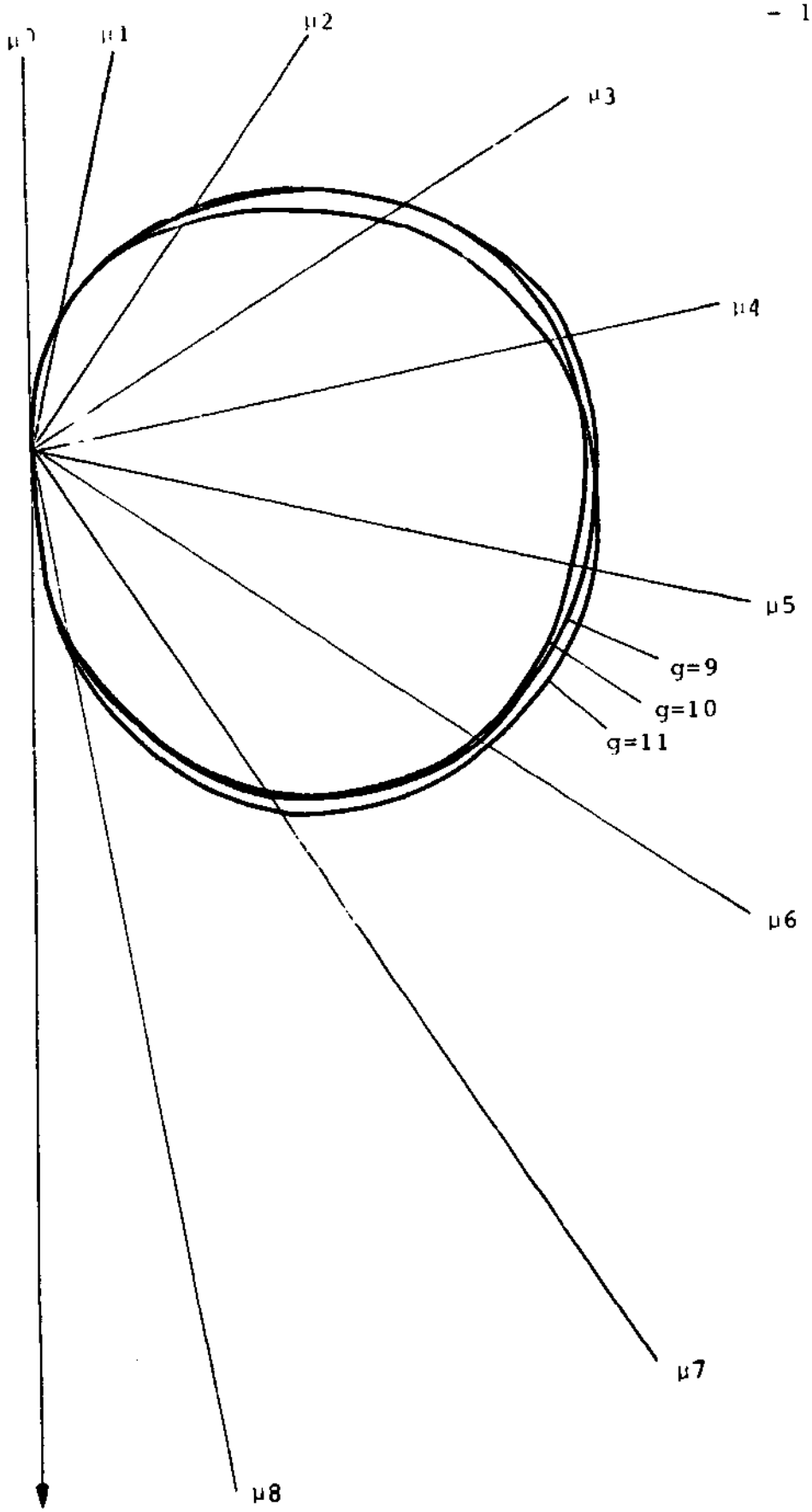

Fig. 6 Directional flux distribution for the energy groups 11 - 9

3.4 Calculating procedure

Three cases were studied independently. Two for the 3-loop HHT design both with and without the boronate graphite wall to examine the effectiveness of this wall in attenuating the neutron flux. The one loop HHT design was studied without wall. In each case the neutron source was devided in four broad energy ranges. Each range was followed separately. In this way it was possible to evaluate the contribution of each energy range to the final results. These partial results were combined taking into account the real population of neutrons per energy range. The calculations were performed in 17 broad energy groups. The first two cases were studied straight forward and for the 3rd case the region restart option was used with increased neutron weight, due to the deep penetration inside the PCRV. For each broad energy range and each direct case $1.2 \cdot 10^5$ neutron were run. The restart option was used at the duct entrance and the first bend. The equivalent amount of source neutrons were $6 \cdot 10^5$.

The dose rate has been calculated for two cases: during reactor operation and two days after shut-down.

For the first case the gamma rays generated through neutron interaction with the materials and those due to core fission products and to impurities were examined. The gamma rays generated through neutron capture and inelastic scattering with all the materials present were stored during the neutron calculation. These were used as source later on to find their transport in the primary circuit and to determine their contribution to the dose rate.

The total value ($2.5 \cdot 10^{11}$ $\gamma/cm^3 s$ for $8 W/cm^3$ core power density) and the spectrum of the gamma rays due to core fission products

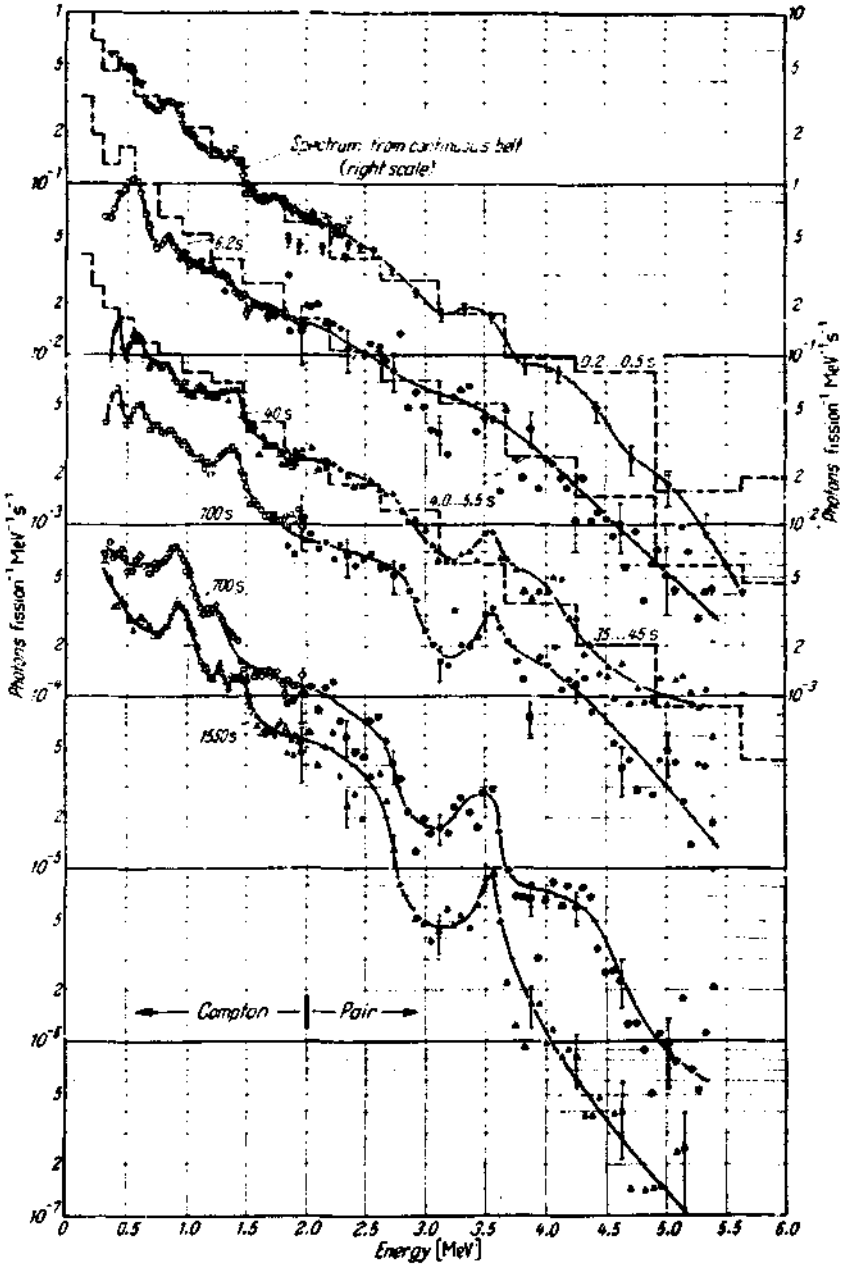

Fig. 2.3.–9b.

Fig. 2.3.–9a and b. Gamma-ray energy spectra for different time intervals after fission of ^{235}U. The points and solid lines are from ORNL studies of thermal fission with two types of multiple-crystal scintillation spectrometers which covered energy regions as indicated in the figure [3, 4]. The histograms are from LASL studies of fission induced by neutrons from a bare critical assembly using a single-crystal scintillation spectrometer with correction for the spectrometer response [5].

Fig. 7 From Ref. (13)

is defined from Ref. (13) and it is given in Fig. 7. This gamma source was used in a separate Monte Carlo simulation of the propagation in the blanket to calculate the flux at the upper level of the gas plenum. In this way we could define a new source and follow the gamma transport in the ducts using the geometry as in Fig.2.

The gamma flux due to impurities (Co in the insulation of the gas plenum, Co, Ta and Hf in the duct walls) was calculated defining the four corresponding sources and running four Monte Carlo cases. The energy of the source photons is given in Table 2 and the angle distribution was assumed isotropic. The source strength has been calculated taking into account the concentration (see Table 3) of the radionuclides and their properties (half lives, activation cross sections) and the neutron fluxes (see Ref. (14)). On this way the results could be used for other impurities concentration (see Table 3). The gamma flux due to the impurities of turbine materials was computed applying the half space assumption.

In the second case (two days after shut-down) the dose rates due to activation of all the materials, impurities and core fission products at this time contribute to the total rate and a similar procedure as explained above was used. For the gamma flux due to the core fission products the corresponding data have been taken from Fig.7. The energy dependent factors used to convert the gamma flux to dose rate were taken from Ref.(13).

Table 2 Calculated source strength per unit volume $\left(\frac{\text{gamma}}{\text{cm}^3 \cdot \text{sec}}\right)$

Nuclide	Energy (MeV)	Insulation	Horizontal duct	Vertical duct
Fe^{58}	0.191	$2.03 \cdot 10^3$	$1.56 \cdot 10^4$	$3.77 \cdot 10^2$
	1.29	$2.9 \cdot 10^4$	$2.24 \cdot 10^5$	$5.41 \cdot 10^3$
	1.1	$3.85 \cdot 10^4$	$2.77 \cdot 10^5$	$7.17 \cdot 10^3$
Cr^{50}	0.32	-	$1.45 \cdot 10^6$	$3.5 \cdot 10^4$
Mo^{99}	0.78	-	$8.02 \cdot 10^4$	$1.94 \cdot 10^3$
	0.74		$6.02 \cdot 10^4$	$1.45 \cdot 10^3$
	0.355		$1.0 \cdot 10^4$	$2.42 \cdot 10^2$
	0.04		$5.0 \cdot 10^5$	$1.21 \cdot 10^4$
	0.18		$6.1 \cdot 10^4$	$1.47 \cdot 10^3$
Co^{60}	1.17	$6.55 \cdot 10^6$	$1.32 \cdot 10^6$	$3.19 \cdot 10^4$
	1.13	$6.55 \cdot 10^6$	$1.32 \cdot 10^6$	$3.19 \cdot 10^4$
Ta^{182}	0.229	-	$3.65 \cdot 10^5$	$8.82 \cdot 10^3$
	0.1		$5.3 \cdot 10^5$	$1.28 \cdot 10^4$
	0.084		$4.46 \cdot 10^5$	$1.08 \cdot 10^4$
	1.281		$7.6 \cdot 10^5$	$1.84 \cdot 10^4$
Hf^{181}	0.482	-	$3.32 \cdot 10^6$	$8.02 \cdot 10^4$
	0.137		$4.1 \cdot 10^6$	$9.9 \cdot 10^4$
	0.346		$4.91 \cdot 10^5$	$1.19 \cdot 10^4$

* For
with
wall
shou
lise
rati

Table 3.: Densities used in the calculation of source strength

The atom densities for impurities were calculated assuming a density of 7.6 gr/cm^3

Nuclide	Insulation	Duct wall	Turbine
Fe	$2.5 \cdot 10^{-3}$ $\frac{at}{b \cdot cm}$	$4.7 \cdot 10^{-2}$ $\frac{at}{b \cdot cm}$	$8.2 \cdot 10^{-2}$ $\frac{at}{b \cdot cm}$
Cr	-	$6.14 \cdot 10^{-3}$ $\frac{at}{b \cdot cm}$	$9.07 \cdot 10^{-4}$ $\frac{at}{b \cdot cm}$
Mo	-	$3.76 \cdot 10^{-3}$ $\frac{at}{b \cdot cm}$	$1.97 \cdot 10^{-4}$ $\frac{at}{b \cdot cm}$
Hf	-	10'000 ppm	10'000 ppm
Ta	-	400 ppm	1'000 ppm
Co	1'000 ppm	200 ppm	500 ppm

4. Presentation of the results

The total neutron flux is given in Fig.8 to Fig.10 as a function of the duct length, for the three calculated cases. The most important component of the source is due to thermal neutrons, (.32 eV $\leq E_{th} \leq$ 2.38 eV) since they constitute 98% of the total flux. The epithermal neutrons, (2.38 eV $\leq E_{ep} \leq$ 111 keV) constitute 1.77%, while the intermediate (111 keV $\leq E_{int} \leq$ 821 keV) and the fast neutrons (821 keV $\leq E_{fast} \leq$ 14.9 Mev) are only 0.11% and 0.08% of the total flux.

The plotted results have the typical shape of neutron fluxes in multilegged ducts. The thermal neutrons remain the dominating component of the total flux, even at high penetrations.

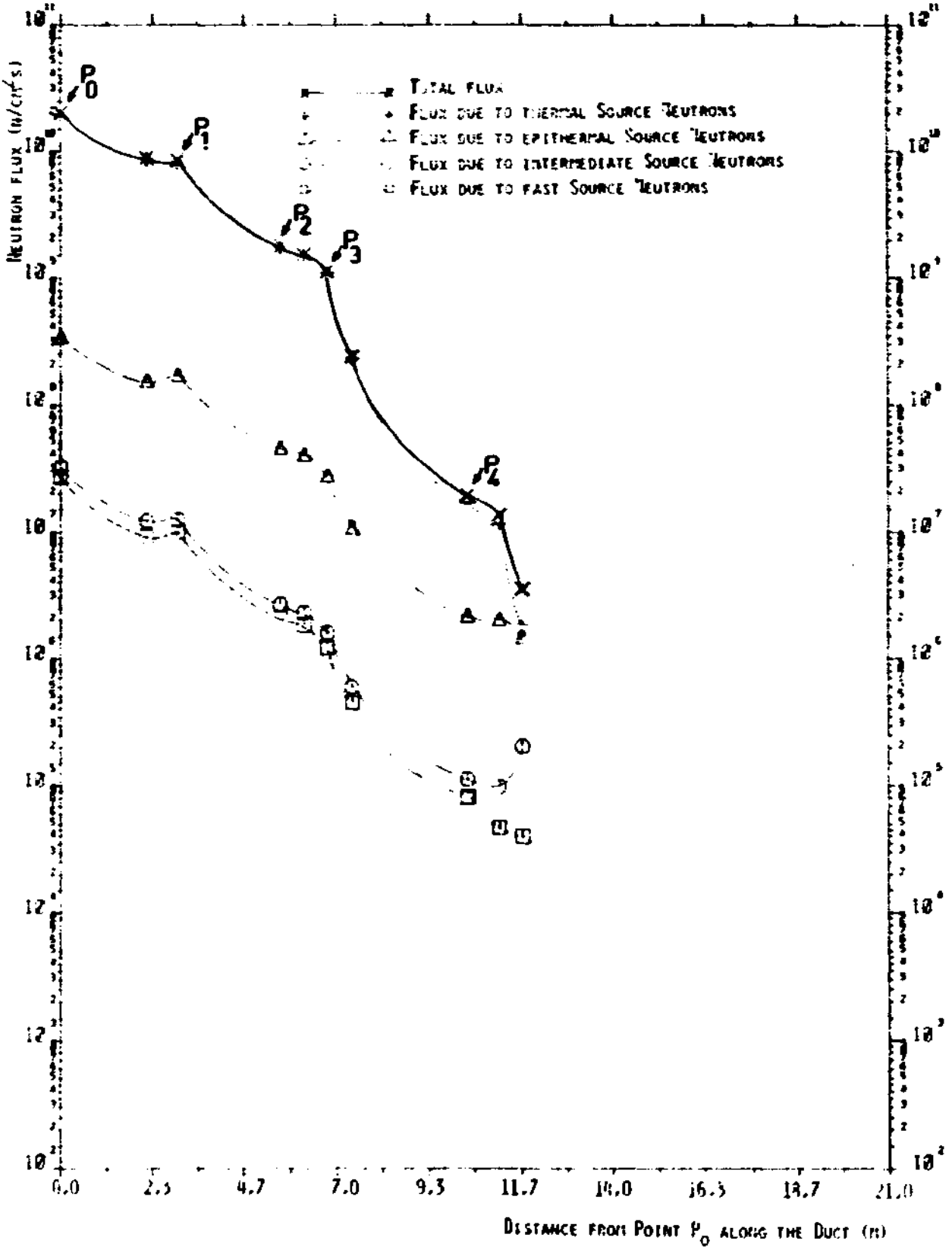

Fig. 8 Total neutron flux as a function of duct length, HHT -3 loop design. Case without wall

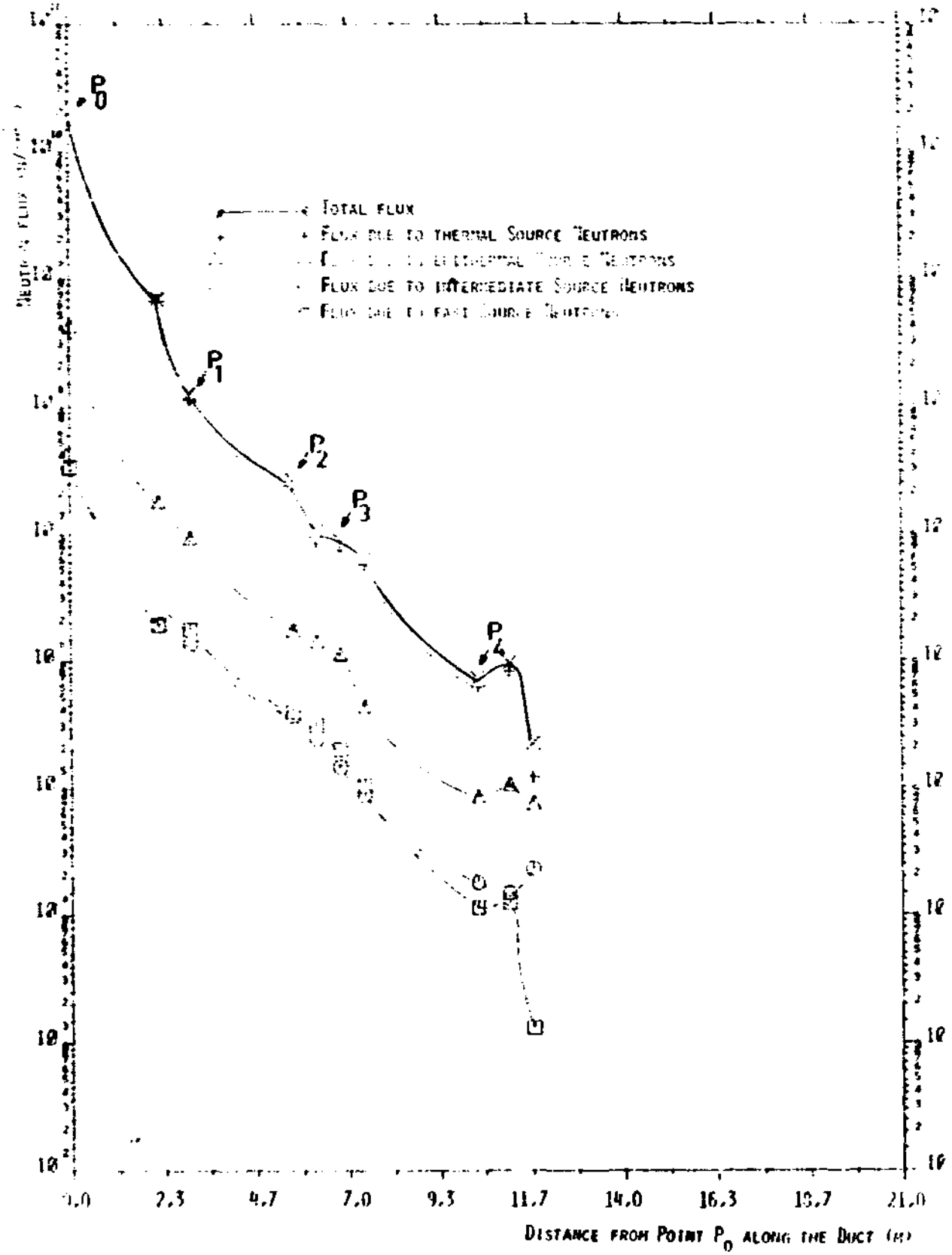

Fig. 9 Total neutron flux as a function of duct length, HHT -3 loop design. Case without wall

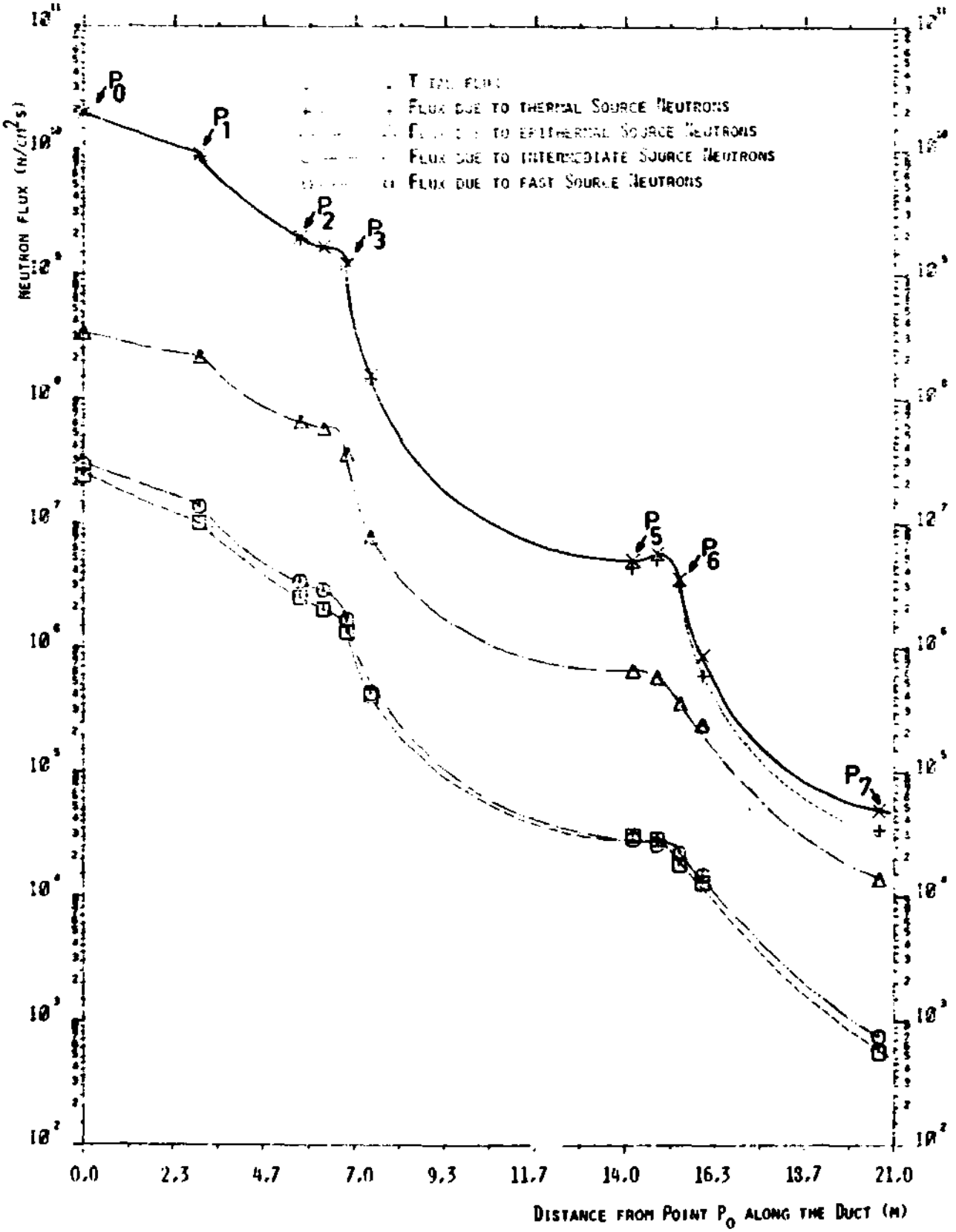

Fig. 10 Total neutron flux as function of duct length, HHT -1 loop design

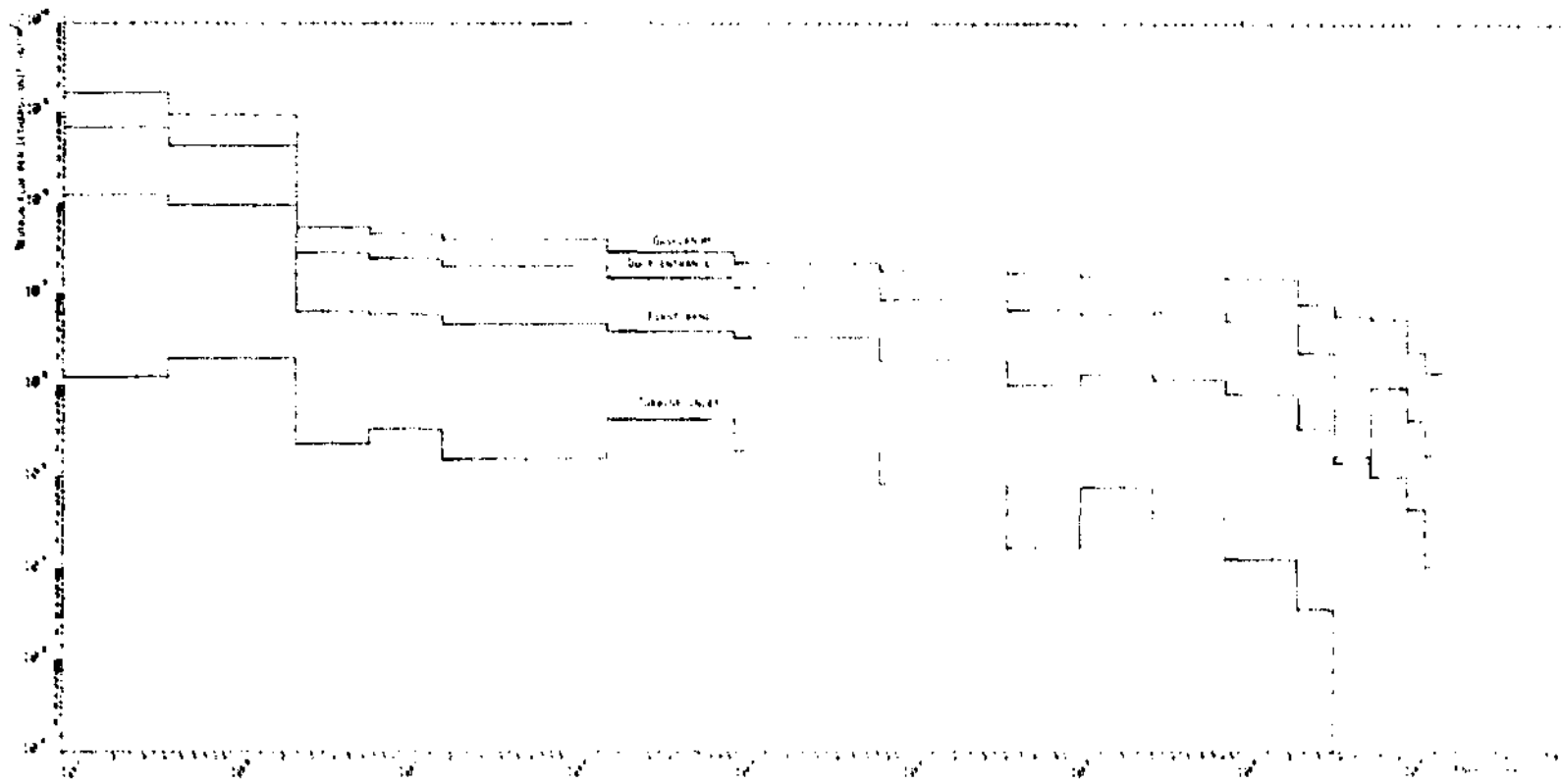

Fig. 11 Neutron spectrum of total flux for different position in the duct. MHT -3 loop design. Case without wall

Fig. 12 Neutron spectrum of total flux for different position in the duct. HHT -3 loop design. Case with wall

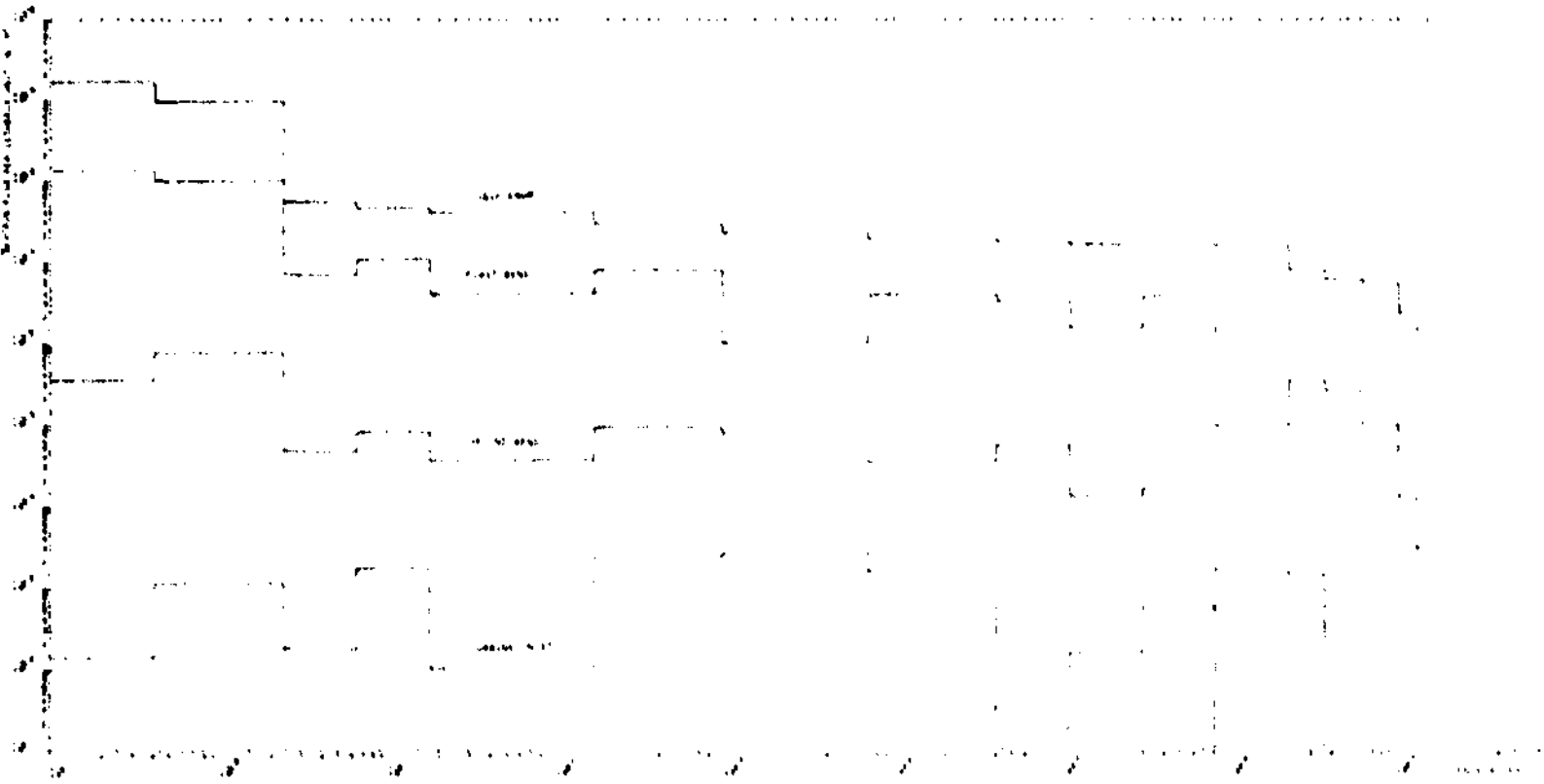

Fig. 13 Neutron spectrum of total flux for different positions in the duct. HHT one loop design

The epithermal neutrons show an increasing importance with penetration and they contribute by 30% to 40% of the flux calculated at the turbine in both cases. The importance of the faster source groups also increases.

The shielding wall attenuates the total flux by an order of magnitude higher. The effect of the wall decreases with increasing energy. The total attenuation from the source to the turbine inlet is 1000 for the case without wall and increases to 30'000 for the case with wall. In the third case, the flux is attenuated by five to six orders of magnitude. This is due to the double bend and the longer ducts of the hot gas pipe. The higher attenuation occurs in the thermal source.

Fig.11 to Fig.13 give the spectrum of the total neutron flux per lethargy unit, for different positions in the ducts. These figures show again the attenuation of the total flux along the ducts and the thermalization of the spectrum. It is interesting to notice the effect of the boronated wall (see Fig.12).It absorbes significally the thermal neutrons and modifies the faster part of the spectrum. On the other hand, in the case without wall the shape remains unchanged between the gas plenum, the duct entrance and the first bend.

The total dose rate for the case during operation is given in Fig.14. The total attenuation, between the gas plenum and the turbire inlet, is relatively small in comparison to the neutron flux attenuation. It varies between $3.4 \cdot 10^4$ for the case with wall and $3.8 \cdot 10^4$ for the case with the double bend. In the case without wall it is only 30. The contribution of each component for the cases during operation and two days after shut-down is explained in details in Table 4 and Table 5.

To determine the statistical error in the calculations, the source was divided in 25 groups of neutrons and the contribution of each group to the region track length was stored

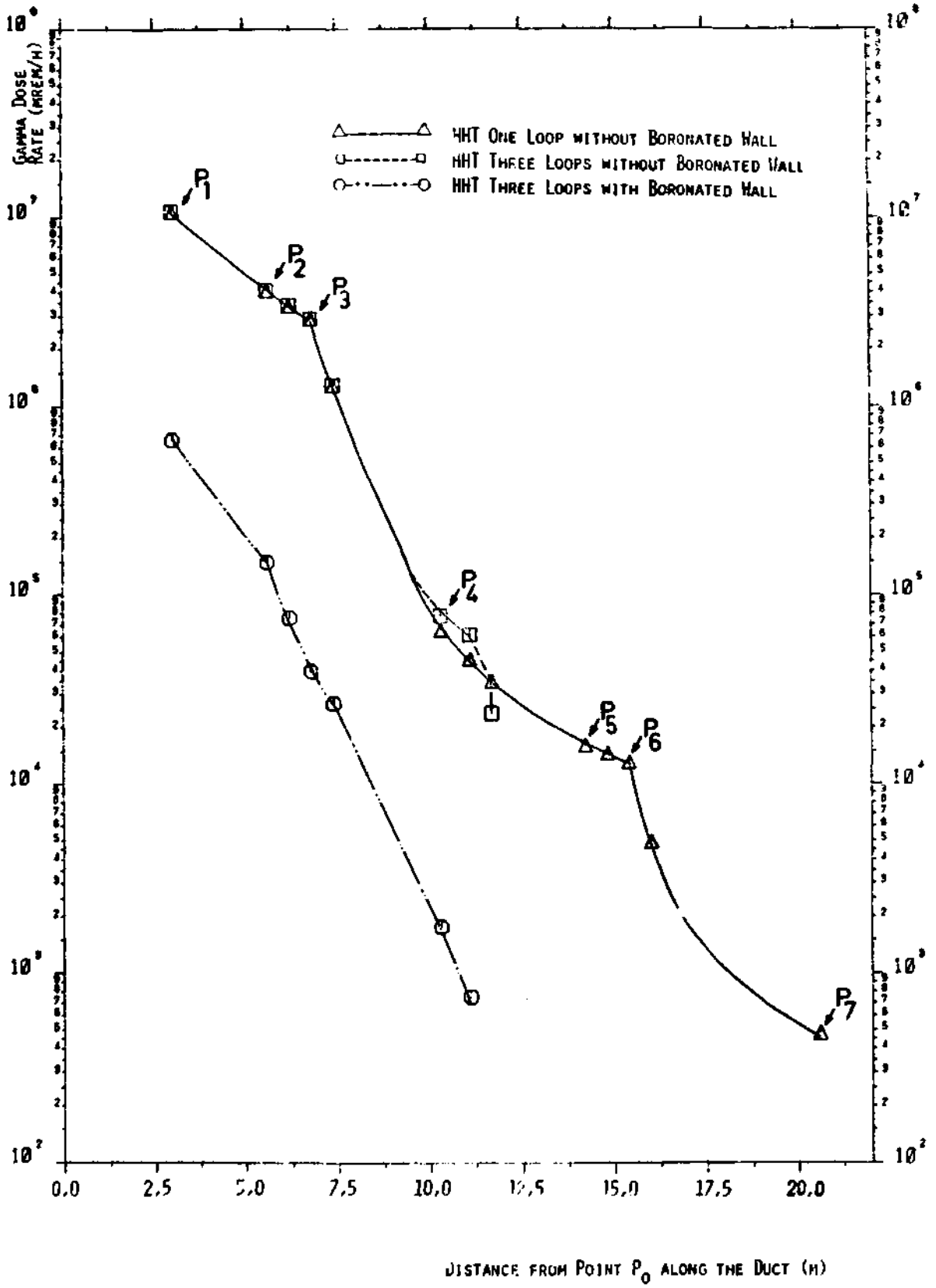

Fig. 14 Total absorbed dose rate during reactor operation

		P_1		P_2		P_4	
		*	**	*	**	*	**
Capture and inelastic scattering of neutrons (mrem/h)		$7 \cdot 10^5$	10^7	$1.5 \cdot 10^5$	$4 \cdot 10^6$	$1.8 \cdot 10^3$	$7 \cdot 10^4$
Fission products (mrem/h)		96	2600	4.2	465	-	1.9
Impurities	Co in the Insulation (mrem/h)	22'000	52'000	178	2000	1	50
	Co in the duct walls (mrem/h)	152	7400	98	4700	3.6	156
	Ta in the duct walls (mrem/h)	48.6	2330	31.4	1530	1.2	54.6
	Hf in the duct walls (mrem/h)	81	3920	68	3300	2	92
	in the turbine (mrem/h)	-	-	-	-	5	67.3
Total rem/h		~ 722	~10'000	~150	~4000	~1.8	~ [illegible]

Table 4 Gamma dose rates due to the different irradiation sources during reactor operation for the cases with (*) and without (**) shielding wall.

		P_1		P_2		P_4	
		*	**	*	**	*	**
Activation of materials components (mrem/h)		104	2550	40	1900	1.5	68
Fission products (mrem/h)		-	1.3	-	1.0	-	-
Impurities	Co in the Insulation (mrem/h)	22'000	52'000	178	2000	1.0	50
	Co in the duct walls (mrem/h)	152	7400	98	4700	3.6	156
	Ta in the duct walls (mrem/h)	48	2300	31	1500	1.2	54
	Hf in the duct walls (mrem/h)	79	3800	66	3200	2	89
Material of the turbine (mrem/h)		-	-	-	-	5.5	74
Total mrem/h		~22'000	~68'000	413	~13'300	14.8	491

Table 5 Gamma dose rates due to the different irradiation sources two days after shut down for the cases with (*) and without (**) shielding wall.

and analysed separately. The variance of the partial results from their mean value, was calculated and the Shapiro-Wilk [15] test of normality was performed. Normality was found until the first bend. Using the student distribution and demanding 90% confidence level, the following results were found for the total neutron flux. The confidence interval was increasing from 1% at the gas plenum to 6% before the bend. It was 10% after the bend, 50% at the turbine inlet and 60% in the turbine wings.

In the case with shielding wall, the results show a higher error. The confidence interval is 50% after the first bend and increases to 80% at turbine inlet. In the third case, where the region restart option was used, the confidence interval was 2% at the duct entrance, 40% after the first bend and it was increasing to 95% at the turbine inlet.

Apart of the statistical error, some other errors should be taken into consideration. The Monte Carlo source used has a systematic error, since it is determined by one dimensional transport calculations. The fact that the cross-section libraries used are collapsed only once in 17 groups, results in systematic errors which require sensitivity analysis to be determined.

Also the upscattering option of FMCEIR could have been used to simulate more accurately the thermal energy range.

5. Conclusions

The essential contribution to the total dose rate during reactor operation is due to the secondary gamma rays.

In the case of 48 hours after shut-down the different contributions of each irradiation source have the same order of magnitude. Only the contribution of the gamma rays generated through fission products in the core is irrelevant. The Co impurity in the insulation of the gas plenum gives the most important part of the dose rate at the duct entrance. In the vertical duct and in the turbine the Co impurity of the duct walls gives a relative higher contribution to the total dose rate.

The total dose rate at the turbine remains always below the limit of 2.5 rem/h, which ensures its accessibility two days after shut-down. This conclusion emphasizes that the shielding wall is not necessary for reducing the irratiation in the turbine. On the other hand the shielding wall is maybe necessary to ensure acceddibility of the first bend. The Plate-out problem of course remains open. More detailed studies are not justified at present, since the HHT project has not yet reached definite designs stage.

References

1. J.J. Loecher, J.E. MacDonald, "Flexible Monte Carlo Programm FMC-N and FMC-G", General Electric APEX 706

2. A. Taormina, "Das Monte Carlo Programm FMCEIR", TM-ST-379, EIR internal report, March 1976

3. B.J. Toppel, A.L. Rago, O.M. O'Shea, "MC2, A Code to Calculate Multigroup Cross Sections", ANL-7318, June 1967

4. J. Patry, Vorbereitung der Wirkungsquerschnitte für das Monte Carlo Programm FMC-N, TM-PH-507, 2.7.1974

5. P. Stiller, Erstellung einer Gruppendatenbibliothek für thermische Neutronen mit der Programmfolge WQTHERM für das Monte Carlo Programm FMCEIR, TM-ST-466, 7.3.1977

6. D.J. Dudziak, "LAPHANO: A Po Multigroup Photon-Production Matrix and Source Code for ENDF", USAEC, Report LA-4750-MS, September 1973

7. P. Stiller, Darstellung einer mit dem Code LAPHAN erzeugten Gammaproduktionsbibliothek für FMCEIR durch das Programm GAMPROD, TM-ST-482, 10.3.1977

8. R.J. Knight, F.R. Mynatt, "MUG: A Program for Generating Photon Cross Sections", CTR-17, Union Carbide Corporation, January 1970

9. P. Stiller, Bereitstellung von Gammawechselwirkungs-querschnitten mit dem Programm SMUG-F für FMCEIR, TM-ST-465, 16.2.1977

10. S. Kypreos, Neutron streaming along Sodium ducts, TM-ST-419, 30.7.1976

11. A. Taormina, Berechnung der Gammaflüsse und der Dosisleistung aus einer Co^{60} Quelle in einer geknick-ten Leitung und Vergleich mit einem Experiment, TM-ST-468, 17.2.1977

12. S. Kypreos, Calculation of fast and thermal neutron fluxes in multilegged ducts and comparison with experiment, TM-ST-470, 8.6.1977

13. R.G. Jaeger, et.al., "Engineering Compendium on Radiation Shielding", Vol 1, Springer Verlag, 1968

14. S. Kypreos, A. Taormina,
Total dose rate calculation in the hot gas duct and the turbine of the HHT during operation and two days after shut-down,
TM-ST-514

15. S. Shapiro, M.B. Wild, "An Analysis of Variance Test for Normality" (Complete Samples), Biometrica 52, 1965